ISSN 0016-7932, Geomagnetism and Aeronomy, 2020, Vol. 60, No. 1, pp. 112–120. © Pleiades Publishing, Ltd., 2020.
Russian Text © The Author(s), 2020, published in Geomagnetizm i Aeronomiya, 2020, Vol. 60, No. 1, pp. 116–125.

Effects of a Short-Term Increase in the Intensity of 630.0-nm Emissions of Atomic Oxygen [OI] at Lower Thermospheric Altitudes due to Anthropogenic Activity

A. V. Mikhalev[a], *, R. V. Vasilyev[a], **, and A. B. Beletskii[a], ***

[a] *Institute of Solar–Terrestrial Physics, Russian Academy of Sciences, Irkutsk, Russia*

**e-mail: mikhalev@iszf.irk.ru*

***e-mail: roman_vasilyev@iszf.irk.ru*

****e-mail: beletsky@mail.iszf.irk.ru*

Received January 21, 2019; revised May 16, 2019; accepted September 26, 2019

Abstract—The paper examines the results of optical observations obtained during Radar Progress experiments to study the effects (the occurrence of extensive, faintly luminous regions and a decrease in plasma concentration) arising from a release of fuel-combustion products from spacecraft engines into the upper atmosphere of the Earth. Analysis of the results of controlled experiments on the injection of "plasma-quenching" compositions into the ionosphere at orbital altitudes indicates that the observed increase in [OI] 630.0-nm intensity in the Radar Progress experiments as a consequence of chemical modification of the ionosphere. The contribution of various components of the injected substance (H_2, OH, H_2O, CO, and CO_2) to the increase in the intensity of atomic oxygen [OI] luminescence at a wavelength of 630.0 nm and to a change in the concentration of the charged component of the upper atmosphere is considered. It is shown that the change in the luminescence intensity and the concentration of the charged component are due to different chemical reactions. The largest contribution to the increase in luminescence intensity is made by the injection of hydrogen and carbon dioxide into the atmosphere, while the decrease in the concentration of plasma particles is mainly caused by the injection of water vapor. It has been found that the characteristic spatiotemporal scales of luminous regions occurring in the upper atmosphere allow them to be recorded by modern spectrophotometric equipment from the Earth's surface without additional information about the time of ignition of the spacecraft engines.

DOI: 10.1134/S0016793220010107

1. INTRODUCTION

The optical luminescence of atomic oxygen in the Earth's atmosphere in the red part of the visible spectrum at a wavelength of 630.0 nm with the forbidden transition $^1D–^3P$ (hereinafter referred to as "[OI] 630.0 nm") occurs under natural conditions at altitudes of 200–300 km, i.e., in the lower thermosphere and *F* region of the ionosphere. Due to the high correlation of the behavior of the [OI] 630.0-nm intensity and the electron concentration (hereinafter, N_e), this emission is often considered a sensitive indicator of changes in the upper atmosphere under the influence of heliogeophysical perturbations or other large-scale geophysical phenomena of various natures: seismic events, wave processes in the atmosphere, etc. Some examples include studies of pulsations in auroras (Eather, 1969), optical flares (Mikhalev and (Beletskii, 2000), midlatitude auroras (Mikhalev et al., 2004), and traveling ionospheric disturbances in the *F* region of the ionosphere (Adachi et al., 2011). It was found that, in addition to natural processes, the [OI] 630.0-nm intensity can also be significantly affected by anthropogenic processes in the ionosphere and thermosphere, in particular, active experiments on heating the ionosphere (Shindin et al., 2017) and the injection of "plasma-quenching" compositions via geophysical rockets (Adushkin et al., 2000), as well as spacecraft (SC) launches and their engine burns during orbital maneuvering (Mendillo et al., 1975; Karlov et al., 1980). Most optical effects related to SC launches and flights are most clearly observed in the troposphere, stratosphere, and mesosphere when large (tens to hundreds kilograms or more) quantities of fuel-combustion products are injected into the atmosphere as a result of burns of liquid propellant engines (hereinafter, "combustion products"). In this case, the observed brightness of the optical glow associated with these events is relatively high (Platov et al., 2003). Optical effects during SC engine burns were also observed at thermospheric altitudes with relatively small amounts of combustion products

injected into the atmosphere (8–9 kg) (Beletskii et al., 2016; Mikhalev et al., 2016). The interpretation of the observed optical effects in these studies was difficult, since there was both the possibility of modification of the ionosphere (Mendillo et al., 1975) accompanied by a decrease in N_e and a simultaneous increase in the [OI] 630.0-nm intensity, as well as the possibility of sunlight scattering on the dispersed component of the combustion products.

In this paper, we consider the possibility of enhancement of the [OI] 630.0-nm intensity as a result of combustion products chemically affecting the components of the upper atmosphere in the Radar Progress experiments. It is believed that the main reactions leading to a decrease in N_e (dissociative recombination reactions) and an increase in [OI] 630.0-nm intensity upon modification of the ionosphere are primarily associated with the injection of H_2O, H_2, and CO_2, which are converted into H_2O^+ and H_2^+, CO_2^+ ions in charge exchange reactions. These ions quickly recombine with free electrons in the ionosphere, and the dissociative recombination rates in reactions involving these ions ("substitution reactions") are orders of magnitude (up to 1000 times) higher than the dissociative recombination rates in reactions on O_2^+ and NO^+ ions in natural conditions.

Intensive exploration of the near-Earth space, accompanied by an increase in the number of SCs and their maneuvering, has led to the need to determine variations in the [OI] 630.0-nm characteristics due to anthropogenic activity in order to separate them from the natural variations in this emission. The primary sign of such artificial variations is the localization of the increase in the [OI] 630.0-nm intensity over the background in time and space. In this paper we study the relationship between the increase in [OI] 630.0-nm intensity, variations in the electron concentration, and the amount of combustion products (H_2, OH, H_2O, CO, and CO_2) released during SC flights in working orbits in the upper atmosphere of the Earth. An additional analysis of the results of optical observations obtained in the Radar Progress experiments (Beletskii et al., 2016; Mikhalev et al., 2016) was performed. The characteristic spatiotemporal scales and the minimum threshold value of the [OI] 630.0-nm intensity accessible for observation by ground-based means under the influence of combustion products were also estimated. The study uses the results of several active experiments on the observation of controlled releases of chemicals at altitudes corresponding to the SC working orbits (Mendillo, 1980; Biondi and Sipler, 1984; Semeter et al., 1996; Beletskii et al., 2016; Mikhalev et al., 2016).

2. RESULTS OF OBSERVATIONS OF INCREASING 630.0-NM EMISSION OF ATOMIC OXYGEN AND DECREASING ELECTRON CONCENTRATION IN VARIOUS EXPERIMENTS

Table 1 gives the results of a series of experiments conducted to study variations in the luminescence of the upper atmosphere and ionospheric plasma concentration under the influence of typical SC fuel combustion products. The researchers monitored the behavior of the amount of injected substance, the [OI] 630-nm intensity, and the electron concentration. Unfortunately, none of the publications on SC launches and flights and active experiments provide the characteristics of the recorded optical effects, the amount and composition of the injected substance, and the magnitude of the variations in N_e at the same time. More complete information on the effects of modification of the ionosphere under the action of the SC engine products can be found in (Mendillo, 1988; Bernhardt et al., 2012).

In the RED AIR 1 and RED AIR 2 experiments (Semeter et al., 1996), equal amounts of CO_2 were injected above and below the maximum height of the night-time $F2$ layer at altitudes with the same N_e value (during sunset, under moonless conditions). In this case, CO_2 interacts with the plasma that has the same electron concentration but different neutral composition and density. Luminous [OI] 630-nm clouds were detected in these experiments as a result of CO_2 injection; their brightness levels are regulated by the quenching processes, and the size of the clouds is determined by the diffusion of the injected substance. In the RED AIR 1 experiment conducted on April 3, 1989, CO_2 was injected with a single rocket at different points along the rocket's flight path. In the RED AIR 2 experiment (December 5, 1991), two rockets with independent CO_2 injection were used, which made it possible to eliminate the cross overlapping of the disturbance regions and to double the mass of the injected substance. Despite the distinct optical effects during CO_2 injection, the accompanying decreases in N_e were smaller than the variations detected by the incoherent scattering radar involved in the RED AIR 1 experiment (less than 6%). Semeter et al. (1996) used this as the basis to argue that, although CO_2 is not an optimal choice for creating ionospheric holes, the photochemical excitation rates of [OI] 630 nm in dissociative recombination of carbon dioxide ions make this process a highly efficient source of luminescence. At the same time, according to the illustration presented in that paper, the RED AIR 2 experiment showed a decrease in N_e at local altitudes of injection from ~30% (248 km) to ~50% (346 km) and the absence of significant changes in N_e in the maximum $F2$ layer.

Table 1. Information on the experiments to study the dynamics of chemical reactions of SC fuel combustion products

Experiment	Mass, kg	Altitude, km	Composition	Δ [OI], R	ΔN_e, %	T, min	Reference
RED AIR 1	9.1	253	CO_2	30	≤ 6	7–10	Semeter et al., 1996
	9.1	379		100	≤ 6		
RED AIR 2	18.4	248	CO_2	525	30	~10	Semeter et al., 1996
	18.4	346		340	50		
BIME Project	42	323	(H_2O and CO_2)	400	–	~5	Biondi and Sipler, 1984
Atlas-Centaur	20000	>200	(H_2O and H_2)	8300	80	~10–20	Mendillo, *Report* ..., 1980
Titan IV B-30	283	0–91	$N_2H_4/N_2H_2(CH_3)_2$	3300	50	~12	Mendillo et al., 2008
	140	73–273	and N_2O_4				
	32	273–494					
Radar-Progress, Progress M-17M	9	412	H_2O, CO_2, H_2, CO	50	–	~2–3	Mikhalev et al., 2016
Radar-Progress, Progress M-23M	8	352	H_2O, CO_2, H_2, CO	50	–	~2–3	Beletskii et al., 2016

In the BIME project (Biondi and Sipler, 1984), 7.4×10^{26} H_2O molecules and 2.7×10^{26} CO_2 molecules (19.7 kg) were injected at an altitude of 323 km. A luminous [OI] 630-nm cloud with an intensity of ~400 R in the central part and a diameter of ~250 km formed ~2 min after the injection of the substance. No data on the N_e behavior are provided in this experiment.

During the launch of the Atlas-Centaur spacecraft, $\sim 7 \times 10^{29}$ H_2O and H_2 molecules were released at an altitude above 200 km. The decrease in N_e near the trajectory reached ~80%. The size of the disturbance region was 2000–3000 km along the track and 600–1000 km across. The [OI] 630-nm intensity at the maximum of the disturbance region amounted to 8300 R. The maximum intensity was observed after several minutes, and 10–20 min later the intensity dropped to the background value (Mendillo, 1980).

Figure 1 shows the dependences of the [OI] 630-nm intensity (hereinafter, we discuss the magnitude of the intensity variations over the background) on the amount of injected substance for various experiments. The results of the experiments indicate that the studied phenomenon shows a tendency of increasing intensity with an increasing amount of injected substance. It can be seen that the intensity increase occurs much faster when only CO_2 is taken into account. The data from the results of the Radar Progress experiments shown in Fig. 1 for comparison with other experiments allow some preliminary conclusions to be drawn. If we compare those taking only the injection of CO_2 molecules into account with the results of the RED AIR 1–2 and BIME experiments, it does not provide the observed increase in the [OI] 630-nm intensity in the Radar Progress experiment (Fig. 1a). However, comparison of the total injected masses (regardless of their composition) in all of the experiments allows the observed increase in intensity to be interpreted as a modification of the ionosphere in this experiment. In other words, the release of combustion products lead to an increase in the number of positively charged molecular ions, which reduces the concentration of electrons and increase the concentration of excited oxygen atoms during dissociative recombination. Based on the results of experiments on the injection of "plasma-quenching" compositions, we can estimate the expected decrease in the electron concentration in the Radar Progress experiments with respect to the magnitude of the increase in the [OI] 630-nm intensity. The expression relating the intensity variation to the variation in the electron concentration based on the experimental data from Table 1 is

$$\ln(\Delta I_{630}) = 0.057\Delta N_e + 4.33, \quad (1)$$

and the regression graph is shown in Fig. 2.

The resulting expression gives the value of ≤1% for ΔN_e at $\Delta I_{630} = 80$ R (the detected value is 40–60 R). Thus, if the nature of the increase in the [OI] 630-nm intensity observed in the Radar Progress experiments coincides with the nature of this phenomenon in other similar experiments, the detection of variations in the electron concentration under the influence of the operation of SC maneuvering engines must be difficult, and the observation of the variations in [OI] 630 nm will be most suitable for remote monitoring of this process. However, the results presented by Shpynev et al. (2017) show that the decrease in N_e in these experiments reaches 20–30% of the background value. This indicates that a decrease in the electron concentration and an increase in the luminescence intensity most likely occur due to different chemical reactions.

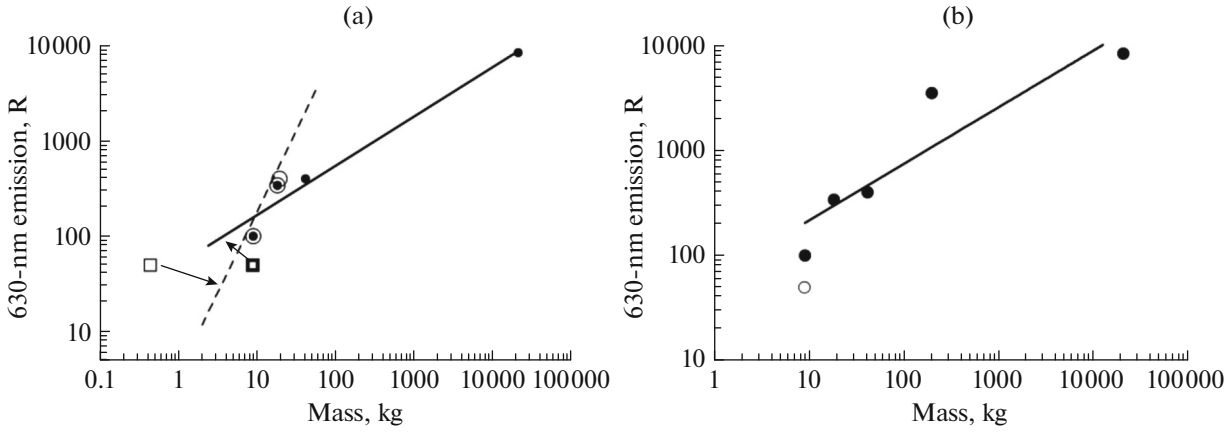

Fig. 1. (a) Comparison of the total injected mass and CO_2 with an increase in the 630-nm emission. The black circles and the solid line (interpolation) show the total mass for four experiments: RED AIR 1, RED AIR 2, the BIME project, and the launch of the Atlas-Centaur spacecraft. The light circles and the dashed line (interpolation) show the mass of CO_2 in the RED AIR 1, RED AIR 2, and BIME project experiments. The dark square is the total mass, and the light square is only the mass of CO_2 in the Radar Progress experiments. (b) Comparison of the total injected mass with an increase in the 630-nm emission. The dark circles and the solid line (interpolation) show the total mass for four experiments: RED AIR 1, RED AIR 2, BIME project, Atlas-Centaur, and Titan IV B-30). The light circle shows the Radar Progress experiments.

3. ESTIMATE OF THE COMPARATIVE EFFECTIVE 630.0-NM EMISSION OF ATOMIC OXYGEN BASED ON REACTIONS INVOLVING H_2, OH, H_2O, CO, AND CO_2 MOLECULES

The population of the spectral level of atomic oxygen $O(^1D)$ under natural conditions mainly occurs as a result of dissociative recombination of molecular oxygen O_2^+ and nitrogen oxide NO^+ ions:

$$O_2^+ + e^- \rightarrow O + O\left(^1D\right), \quad (2)$$

$$NO^+ + e^- \rightarrow N + O(^1D) \quad (3)$$

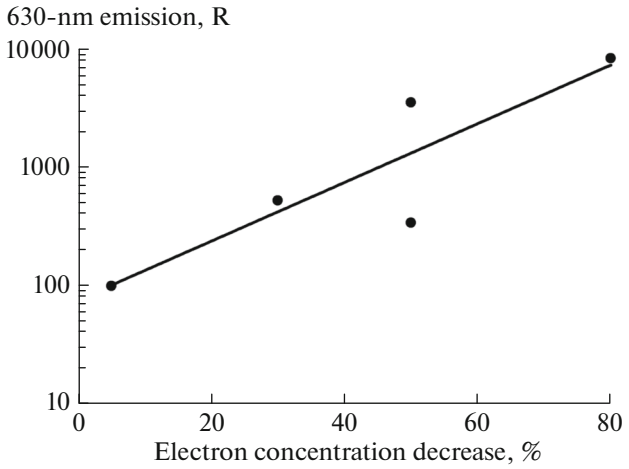

Fig. 2. Relationship between the observed increase in the 630-nm emission and the decrease in electron concentration (in %) in the experiments listed in Table 1.

followed by the spontaneous emission of a quantum of light with a wavelength of 630 nm:

$$O(^1D) \rightarrow O(^3P) + h\nu \text{ (630 nm)} \quad (4)$$

O_2^+ and NO^+ ions are formed in the charge exchange reactions:

$$O^+ + O_2 \rightarrow O_2^+ + O, \quad (5)$$

$$O^+ + N_2 \rightarrow NO^+ + N, \quad (6)$$

the rate coefficients of these reactions are

$$K_2 = 1.95\times10^{-7}\left(300/T_e\right)^{0.7},$$

$$K_3 = 4.2\times10^{-7}\left(300/T_e\right)^{0.85},$$

$$K_5 = 3.2\times10^{-1}\exp[3.7(300/T_i) - 1.9(300/T_i)^2],$$

$$K_6 = 2.8\times10^{-13}\exp[3.1\left(300/T_i\right) - 0.6\left(300/T_i\right)^2]$$

respectively (Mendillo et al., 1993), where T_e is the electron temperature and T_i is the ion temperature. The [OI] 630-nm intensity at night at midlatitudes under unperturbed conditions is 30–100 R.

The natural background for [OI] 630-nm emission during chemical releases in the upper atmosphere is complemented by the emission at this wavelength due to other chemical reactions. The literature cites several reactions that lead to an additional population of the atomic oxygen $O(^1D)$ level and an increase in the [OI] 630.0-nm intensity upon the injection of H_2, OH, H_2O, CO, and CO_2 molecules, which are part of rocket fuel combustion products or are formed in the atmosphere as the fuel burns.

3.1. Reactions Involving Water and Hydroxyl Molecules (H_2O and OH)

According to current views, water molecules at altitudes corresponding to the SC working orbits may participate in the charge exchange reactions, in particular, with a positive oxygen ion (Dressler et al,. 1991; Mendillo et al., 1993):

$$H_2O + O^+ \rightarrow H_2O^+ + O, \quad (7)$$

$$H_2O + O^+ \rightarrow H_2O^+ + O(^1D), \quad (8)$$

which is followed by the emission of a 630.0-nm photon in accordance with (4).

The rate coefficient of reaction (7) is $K_7 = 3.2 \times 10^{-9}$ (Mendillo et al., 1993). Analysis of the kinetic energy of ions in reaction (8) suggests that it can be a minor additional source of [OI] 630 nm. The intensity increases due to the direct excitation of $O(^1D)$ in the charge exchange reaction. However, this reaction has a collision energy threshold of 0.97 eV (Dressler et al., 1991). The probability of this branch is significantly lower than that of (7), and the branching coefficient of reactions (7) and (8) is not known exactly. Zinn et al. (1980) estimate reaction (8) at 5% of reaction (7). In this case, the population of the excited ^1D level (and, as a consequence, an increase in the [OI] 630-nm intensity) may depend on the relative velocity of water molecules and oxygen ions. For a H_2O molecule incident on a conditionally immobile O^+ ion, the collision energy threshold of 0.97 eV corresponds to the velocity of ~3.2 km/s. The rate of expansion of the luminous region in the first seconds after injection in the experiment was 6–7 km/s along the orbit of Progress M-17M and Progress M-23M and 3–3.5 km/s across the orbit. However, the glow persisted for several minutes, and the estimate of the average expansion rates of the luminous regions to maximum size (~250 km) gives values of ~1 km/s (for the experiment with Progress M-23M) and ~1.4 km/s (Progress M-17M). Thus, we can say either that there is no significant contribution of reaction (8) to the [OI] 630-nm intensity in the Radar Progress experiments or that it is negligible and realized only in the first seconds after the SC engine ignition. Interestingly, in the BIME experiment (Biondi and Sipler, 1984), a luminous [OI] 630-nm region formed after the release of 2.7×10^{26} CO_2 molecules and 7.4×10^{26} H_2O molecules in the ionosphere at an altitude of 323 km. The increase in the luminescence intensity reached 400 R 2 min after the release, and the region with increased luminescence intensity reached 250 km in diameter 3 min later. In this case, the values of the average expansion rate of the luminous region (~1.4 km/s) and its characteristic size were close to those obtained in the Radar Progress experiments. In this regard, the comparison of the RED AIR 2 and BIME experiments can serve as an additional argument in favor of the insignificant contribution of reaction (8) to the integrated [OI] 630-nm intensity in the experiments under consideration (Table 1). In these experiments, the response of [OI] 630 nm to the injection of comparable masses of CO_2 (18.4 and 19.8 kg) was also comparable, even though H_2O (22.2 kg) was additionally injected in the BIME experiment.

An H_2O^+ ion is further involved in the recombination reaction

$$H_2O^+ + e^- \rightarrow OH + H. \quad (9)$$

The rate coefficient of reaction (9) is $K_9 = 6.5 \times 10^{-7} (300/T_e)^{0.5}$ (Mendillo et al., 1993). Apparently, it is this reaction that causes a significant decrease in N_e in the region of its occurrence (Table 1, Atlas Centaur experiment). It should be noted that the decrease in the electron density concentration in the Radar Progress experiments reaches 20–30% of the background level (Shpynev et al., 2017), and the lifetime of the perturbed region is tens of minutes, while the lifetime of luminous formations is no more than ten minutes (Beletskii et al., 2016; Mikhalev et al., 2016). This difference between the lifetime of the perturbation in the plasma concentration and the perturbation in the background [OI] 630-nm luminescence also indicates that a decrease in the electron concentration and an increase in the [OI] 630-nm luminescence intensity in the Radar Progress experiments are caused by different chemical reactions.

The emission of the rotational levels of an excited hydroxyl molecule in the (9-3) band that forms as a result of this reaction can, in principle, contribute to the observed increase in optical emission. The $P_2(3)$ line of this band lies close to the 630.0-nm line (629.8 nm), and the use of interference light filters with a ~2-nm band in the studies allows the possibility of the mixing of emission from two sources and hydroxyl emission, which is "disguised" as oxygen emission. However, the maximum intensity of hydroxyl luminescence is realized in the bands in the near-IR range; therefore, the main contribution of reaction (9) in [OI] 630 nm is small, and the main response to the operation of SC engines in this case should be expected in the infrared emission of the atmosphere.

Considering the above, it can be said that the contributions of reactions (8) and (9) to the integrated [OI] 630-nm intensity are apparently insignificant, but reaction (9) is the primary source of the decrease in the electron concentration. Indirect data indicating the possibility of the endothermic charge exchange reaction of water molecules with positively charged atomic oxygen ions, as well as the hypothetical possibility of leakage of the hydroxyl luminescence through the band-pass filter of the recording device, leave open the question of the quantitative contribution of reactions (8) and (9) to the integrated [OI] 630-nm intensity and require additional research.

3.2. Reactions Involving Hydrogen and Carbon Dioxide Molecules (H_2 and CO_2)

Molecular hydrogen and carbon dioxide injected into the upper atmosphere by an SC engine contribute to an increase in [OI] 630 nm by means of process (4). The necessary atomic oxygen in the excited state forms in the sequences of reactions with carbon dioxide:

$$CO_2 + O^+ \rightarrow O_2^+ \rightarrow CO \quad (10)$$

(the rate coefficient is $K_{10} = 9.4 \times 10^{-10}$), and the molecular oxygen ion further participates in dissociative recombination (2).

Molecular hydrogen participates in the ion-exchange process with the formation of a positively charged hydroxyl ion, which decomposes by dissociative recombination into atomic hydrogen and oxygen:

$$H_2 + O^+ \rightarrow OH^+ + H, \quad (11)$$

$$OH^+ + e^- \rightarrow O(^1D) + H, \quad (12)$$

the rate coefficients of these reactions are $K_{11} = 1.7 \times 10^{-9}$ and $K_{12} = 7.5 \times 10^{-8}(300/T_e)^{0.5}$, respectively (Mendillo et al., 1993).

3.3. Reactions Involving Carbon Monoxide and Hydroxyl Molecules (CO and OH)

According to the information in the literature, ion-exchange interaction between atomic oxygen ion and carbon monoxide

$$CO + O^+ \rightarrow CO^+ + O \quad (13)$$

does not occur. Anicich (1993) estimated the maximum rate coefficient for this reaction at $K_{13} < 10^{-13}$. The process of dissociative recombination of a carbon monoxide ion is exothermic:

$$CO^+ + e^- \rightarrow O(^1D) + C \quad (14)$$

(Rosen et al., 1998); the rate coefficient $K_{14} = 2.75 \times 10^{-7}\ (300/T_e)^{0.55}$; the probability of this branch is ~10%. The sequence of reactions (13) → (14), if realized, leads to an increase in the [OI] 630-nm intensity.

The primary mechanism of CO loss for altitudes above 100 km is the recombination reaction via triple collision (Lee et al., 2018):

$$CO + O + M \rightarrow CO_2 + M. \quad (15)$$

In this case, the average lifetime of carbon monoxide at these altitudes is tens of days, which indicates an incomparably slow rate of progress of (15) in comparison with the rate of other reactions.

There is a faster mechanism of chemical loss of CO in the presence of hydroxyl generated in (9) and contained in the combustion products of SC engines (Ryan et al., 2018):

$$CO + OH \rightarrow CO_2 + H, \quad (16)$$

the rate coefficient of the reaction is $K_{16} = 1.5 \times 10^{-13}$ (Nair et al., 1994). The molar composition of the substance used in the Radar Progress–Progress M-17M experiment (Mikhalev et al., 2016) makes it possible to estimate the mass and number of molecules for OH injected into the atmosphere. These values are 2.6×10^{-4} kg or 9.1×10^{21} molecules, respectively. In addition, hydroxyl is formed in reaction (9) from 2.6 kg or 8.8×10^{25} water molecules. The contribution of these sources and the estimation of the volume V of the observed luminous region as a cylinder with a diameter of 300 km and a height of 50 km ($V = 3.5 \times 10^{21}$ cm^3) estimate the hydroxyl concentration in this volume as ~2.5×10^4 cm^{-3} at a comparable concentration of CO: 1.07×10^4 cm^{-3} (Table 2). Therefore, a certain amount of carbon dioxide generated as a result of the sequence (7) → (9) → (16) should, in principle, contribute to an increase in the integrated [OI] 630-nm intensity via (10) → (2). Comparison of the absolute values of the concentration of atomic oxygen (10^9–10^{10}), hydroxyl, and carbon dioxide indicates that this process is very weak due to a decrease in hydroxyl by the reaction

$$OH + O \rightarrow O_2 + H. \quad (17)$$

We have already mentioned the indirect indication of the absence of an increase in the [OI] 630-nm intensity under the influence of injected water only. Since water was the main source of OH in accordance with (7) → (9) during the engine burns in the Radar Progress experiments, the processes similar to the described sequence of charge exchange with an atomic oxygen ion and further dissociative recombination of the product

$$OH + O^+ \rightarrow OH^+ + O \quad (18)$$

and further (12) or

$$OH + O^+ \rightarrow O_2^+ + H \quad (19)$$

followed by (2), which hypothetically contribute to the increase in intensity, are significantly suppressed for hydroxyl.

4. SPATIOTEMPORAL SCALES OF A SHORT-TERM INCREASE IN THE 630.0-NM EMISSION INTENSITY OF ATOMIC OXYGEN

The published data on the dynamics of [OI] 630 nm (Mendillo, 1980; Biondi and Sipler, 1984; Semeter et al., 1996; Mendillo et al., 2008; Mikhalev et al., 2016; Beletskii et al., 2016) show a rather rapid (1–2 min) increase in intensity after the injection of the substance and a relatively slow (5–20 min) decrease. Table 1 shows the characteristic time for the [OI] 630-nm intensity to decrease to half its maximum value ($T_{1/2}$) after the injection of the substance and to reach the maximum luminescence. It is believed that the size of the region of increased luminescence is determined by the diffusion of the injected substance (Semeter et al., 1996).

Table 2. Composition of the injected substance in the Radar Progress experiments

Substance	Percentage, %	Mass, kg	AEM	Number of molecules, units	Concentration in the luminous region, m^{-3}
H_2O	2.93×10^{-1}	2.6388	18	8.83×10^{25}	2.52×10^{4}
N_2	2.68×10^{-1}	2.4084	28	5.18×10^{25}	1.48×10^{4}
CO	1.93×10^{-1}	1.7388	28	3.74×10^{25}	1.07×10^{4}
H_2	1.88×10^{-1}	1.6893	2	5.09×10^{26}	1.45×10^{5}
CO_2	4.95×10^{-2}	0.44514	44	6.09×10^{24}	1.74×10^{3}
H	8.52×10^{-3}	0.076716	1	4.62×10^{25}	1.32×10^{4}
NO	3.39×10^{-4}	0.0030528	30	6.13×10^{22}	1.75×10^{1}
OH	2.85×10^{-5}	0.00025677	17	9.10×10^{21}	2.60×10^{0}
O_2	2.74×10^{-5}	0.00024696	32	4.65×10^{21}	1.33×10^{0}
O	1.39×10^{-5}	0.00012519	16	4.71×10^{21}	1.35×10^{0}
N	5.38×10^{-8}	0.00000048	14	2.08×10^{19}	5.95×10^{-3}

Table 3. Comparison of the contribution of various processes to the variation in the atomic oxygen luminescence intensity at a wavelength of 630.0 nm and the plasma concentration

Parameter	O_2 (natural conditions)	H_2O	CO_2	H_2	CO	OH
[OI] 630.0 nm	$K_4K_2 \sim 6 \times 10^{-19}$ $k = 1$	K_8 –? k –? (slightly)	$K_{10}K_2 \sim$ $\sim 1.8 \times 10^{-16}$ $k \sim 300$	$K_8K_9 \sim$ $\sim 1.3 \times 10^{-16}$ $k \sim 220$	$K_{13}K_{14} \sim 10^{-20}$ $k \sim 0.1$ $K_{16}K_{10}K_2 \sim 10^{-29}$ $k \sim 10^{-10}$	K_{18} –? k –? (insignificantly) K_{19} –? k –? (insignificantly)
N_e	$K_4K_2 \sim 6 \times 10^{-19}$ $k = 1$	$K_7K_9 \sim 2.1 \times 10^{-15}$ $k \sim 3500$	$K_{10}K_2 \sim$ $\sim 1.8 \times 10^{-16}$ $k \sim 300$	$K_8K_9 \sim$ $\sim 1.3 \times 10^{-16}$ $k \sim 220$	$K_{13}K_{14} \sim 10^{-20}$ $k \sim 0.1$	K_{18} –? k –? (insignificantly) K_{19} –? k –? (insignificantly)

The minimum size of the region of increased [OI] 630-nm luminescence in the analyzed studies was 250–270 km, which corresponds to sufficiently large visible angular sizes of 35°–40° (for luminescence altitudes of 300–400 km). The estimated (Mikhalev et al., 2016; Beletskii et al., 2016) variation in the [OI] 630-nm intensity at 40–60 R (with a transverse size of 250–350 km upon the injection of 9 kg of SC engine product) is comparable to the natural level of this emission at night at midlatitudes under quiet geomagnetic conditions. The detection of variations in [OI] 630 nm within 10–20% of its natural level under good weather conditions is the norm, and modern specialized optical systems are capable of detecting variations in the 630-nm line emission as small as units of Rayleighs. Therefore, we can expect the possibility of detecting the SC engine burn in the atmospheric glow, even with lower masses of the injected substance than those considered in this paper. In this case, the expected luminescence intensities, the size of the luminous region, and the characteristic times of [OI] 630-nm luminescence can be much smaller and equal to units of Rayleighs, tens of kilometers, and tens of seconds, respectively.

Table 3 shows the conditional values of the efficiencies of the above processes for the excitation (additional enhancement) of [OI] 630 nm and a decrease in N_e as compared with natural conditions. The conditional efficiency was determined via multiplication of the corresponding reaction rate coefficients. Index k shows the effectiveness of the corresponding reactions as compared to natural conditions, for which k is taken as 1.

Naturally, the expected effects of an increase in [OI] 630 nm and a decrease in N_e depend on the amount and composition of the injected substance, the altitude of injection, and other geophysical factors. It should also be noted that the defining reactions for these two effects may be different. For example, Table 3 shows

that the effect of a decrease in the plasma concentration among the molecules under consideration is caused by reactions involving H_2O water molecules, while reactions involving CO_2 and H_2 molecules are determinant for an increase in [OI] 630 nm. In this case, the contribution of CO to the increase in intensity via interaction with OH injected and generated by water is not significant.

Table 2 provides information on the chemical composition of the substance used in the Radar Progress experiments. With comparable efficiencies of the reactions that increase the [OI] 630.0-nm intensity by CO_2 and H_2 molecules, the number of injected H_2 molecules significantly (by at least several times) exceeds the total number of H_2O, CO_2, CO, and OH molecules. This suggests that reactions (11) and (12) involving H_2 molecules are decisive in the [OI] 630-nm intensification in Radar Progress experiments. As for other processes, although they contribute to the increase in intensity, their effect is insignificant as compared to the action of hydrogen.

5. CONCLUSIONS

The studies determined the relationship between an increase in the [OI] 630-nm intensity, a decrease in the electron concentration, and the released mass of H_2O, H_2, CO, and CO_2 during the injection of fuel combustion products upon the ignition of SC engines at altitudes of their working orbits. Additional analysis of the optical results in the Radar Progress experiments was carried out with a small amount of injected substance (Beletskii et al., 2016; Mikhalev et al., 2016). The minimum threshold value of the [OI] 630-nm intensity accessible for observation by ground-based means and the expected characteristic spatiotemporal scales of luminescence during the injection of the products of the SC engines at thermospheric altitudes was estimated. In particular, the following preliminary results were obtained.

(1) Analysis of the results of experiments on the injection of "plasma-quenching" compositions into the ionosphere at the altitudes of the working orbits of SCs allows the assumption that the observed increase in the [OI] 630.0-nm intensity in Radar Progress experiments is the result of chemical reactions in the upper atmosphere, which lead to an increase in the concentration of atomic oxygen in the $O(^1D)$ state.

(2) Evaluation of the comparative efficiency of an increase in the [OI] 630.0-nm intensity for reactions involving H_2, H_2O, CO, and CO_2 molecules showed that the increase in the [OI] 630.0-nm intensity observed in the Radar Progress experiments was mainly caused by reactions (11) and (12) involving H_2 molecules. The most efficient decrease in the electron concentration in these experiments occurs in reactions (7) and (9) involving H_2O molecules.

(3) During the operation of correcting SC engines in near-Earth orbits or injection of "plasma-quenching" compositions at lower thermospheric altitudes with a total mass of injected substance $\leq$10 kg, the [OI] 630.0-nm intensity may increase to 10–50 R above the background value. The characteristic sizes of luminous regions reach tens and hundreds kilometers, and the lifetimes of these formations are tens and hundreds seconds. These parameters indicate the accessibility of these events for detection by ground-based observational means.

It will be useful to take these results into account in studies of fast optical phenomena in the Earth's atmosphere (see, e.g., Mikhalev and Beletskii, 2000; Yair et al., 2005; Yang et al., 2014).

6. ACKNOWLEDGMENTS

The observation results were obtained with the use of the equipment of the Angara Collective Use Center (http://ckp-rf.ru/ckp/3056/).

FUNDING

This study was supported by the Russian Foundation for Basic Research, project no. 17-05-00492, and as part of basic funding for the fundamental scientific research program FSR II.16.

REFERENCES

Adachi, T., Otsuka, Y., Yamaoka, M., Yamamoto, M., Shiokawa, K., Chen, B., and Hsu, R., First satellite-imaging observation of medium-scale traveling ionospheric disturbances by FORMOSAT-2/ISUAL, *Geophys. Res. Lett.*, 2011, vol. 38, L04101. https://doi.org/10.1029/2010GL046268

Adushkin, V.V., Kozlov, S.I., and Petrov, A.V., *Ekologicheskie problemy i riski vozdeistviya raketno–kosmicheskoi tekhniki na okruzhayushchuyu sredu: Spravochnoe posobie* (Ecological Problems and Risks of the Environmental Impact of Rocket and Space Equipment: A Handbook), Moscow: Ankil, 2000.

Anicich, V.G., Evaluated bimolecular ion–molecule gas phase kinetics of positive ions for use in modeling planetary atmospheres, cometary comae, and interstellar clouds, *J. Phys. Chem. Ref. Data*, 1993, vol. 22, no. 1469. https://doi.org/10.1063/1.555940

Beletsky, A.B., Mikhalev, A.V., Khakhinov, V.V., and Lebedev, V.P., Optical effects produced by running onboard engines of low-Earth-orbit spacecraft, *J. Sol.-Terr. Phys.*, 2016, vol. 2, no. 4, pp. 107–117. https://doi.org/10.12737/24277

Bernhardt, P.A., Ballenthin, J.O., Baumgardner, J.L., et al., Ground and space-based measurement of rocket engine burns in the ionosphere, *IEEE Trans. Planet. Sci.*, 2012, vol. 40, no. 5, pp. 1267–1285.

Biondi, M.A. and Sipler, D.P., Studies of equatorial 630.0 nm airglow enhancements produced by a chemical release in the *F*-region, *Planet. Space Sci.*, 1984, vol. 32, no. 12, pp. 1605–1610.

Dressler, R.A., Gardner, J.A., Cooke, D.L., and Mirad, E., Analysis of ion densities in the vicinity of space vehicles' non-neutral chemical kinetics, *J. Geophys. Res.*, 1991, vol. 96, no. A8, pp. 13795–13806.

Eather, R.M., Short-period auroral pulsations in 6300 A OI, *J. Geophys. Res.*, 1969, vol. 74, no. 21, pp. 4998–5004.

Karlov, V.D., Kozlov, S.I., and Tkachev, G.N., large-scale ionospheric disturbances caused by the flight of a rocket with operating engine, *Kosm. Issled.*, 1980, vol. 18, no. 2, pp. 266–277.

Lee, J.N., Wu, D.L., Ruzmaikin, A., and Fontenla, J., Solar cycle variations in mesospheric carbon monoxide, *J. Atmos. Sol.-Terr. Phys.*, 2018, vol. 170, pp. 21–34. https://doi.org/10.1016/j.jastp.2018.02.001

Mendillo, M.J., Report on investigations of atmospheric effects due to HEAO-C launch, *AIAA Pap.*, 1980, no. 888, pp. 1–5. https://doi.org/10.2514/6.1980-888

Mendillo, M., Ionospheric holes: A review of theory and recent experiment, *Adv. Space Res.*, 1988, vol. 8, no. 1, pp. 51–62.

Mendillo, M.J., Hawkins, G.S., and Klobuchar, J.A., A sudden vanishing of the ionospheric *F* region due to the launch of Skylab, *J. Geophys. Res.*, 1975, vol. 80, no. 16, pp. 2217–2218.

Mendillo, M., Semeter, J., and Noto, J., Finite element simulation (FES): A computer modeling technique for studies of chemical modification of the ionosphere, *Adv. Space Res.*, 1993, vol. 13, no. 10, pp. 55–64.

Mendillo, M., Smith, S., Coster, A., Erickson, P., Baumgardner, J., and Martinis, C., Man-made space weather, *Space Weather*, 2008, vol. 6, no. 9, S09001. https://doi.org/10.1029/2008SW000406

Mikhalev, A.V. and Beletsky, A.B., Characteristics of optical flares in night-time atmospheric radiation according to data of observations with a multispectral photometer and a TV-camera, *Opt. Atmos. Okeana*, 2000, vol. 13, no. 4, pp. 338–341.

Mikhalev, A.V., Beletsky, A.B., Kostyleva, N.V., and Chernigovskaya, M.A., Midlatitude auroras in the south of Eastern Siberia during strong geomagnetic storms on October 29–31, 2003 and November 20–21, 2003, *Cosmic Res.*, 2004, vol. 42, no. 6, pp. 591–596.

Mikhalev, A.V., Khakhinov, V.V., Beletsky, A.B., and Lebedev, V.P., Optical effects of the operation of the onboard engine of the *Progress M-17M* spacecraft at thermospheric heights, *Cosmic Res.*, 2016, vol. 54, no. 2, pp. 105–110.

Nair, H., Allen, M., Anbar, A.D., Yung, Y.L., and Clancy, R.T., A photochemical model of the Martian atmosphere, *Icarus*, 1994, vol. 111, no. 1, pp. 124–150. https://doi.org/10.1006/icar.1994.1137

Platov, Yu.V., Kulikova, G.N., and Chernous, S.A., Classification of Gas-Dust Structures in the Upper Atmosphere Associatedwith the Exhausts of Rocket-Engine Combustion Products, *Cosmic Res.*, 2003, vol. 41, no. 2, pp. 153–158.

Rosen, S., Peverall, R., Larsson, M., Padellec, A., Semaniak, J., Larson, A., Stromholm, C., Zande, W.J., Danared, H., and Dunn, G.H., Absolute cross sections and final-state distributions for dissociative recombination and excitation of $CO^+(v = 0)$ using an ion storage ring, *Phys. Rev. A*, 1998, vol. 57, no. 6, pp. 4462–4471. https://doi.org/10.1103/PhysRevA.57.4462

Ryan, N.J., Kinnison, D.E., Garcia, R.R., Hoffmann, C.G., Palm, M., Raffalski, U., and Notholt, J., Assessing the ability to derive rates of polar middle-atmospheric descent using trace gas measurements from remote sensors, *Atmos. Chem. Phys.*, 2018, vol. 18, pp. 1457–1474. https://doi.org/10.5194/acp-18-1457-2018

Semeter, J., Mendillo, M., Baumgardner, J., Holt, J., Hunton, D.E., and Eccles, V.A., Study of oxygen 6300 airglow production through chemical modification of the nighttime ionosphere, *J. Geophys. Res.*, 1996, vol. 101, no. A9, pp. 19683–19699.

Shindin, A.V., Klimenko, V.V., Kogogin, D.A., Beletsky, A.B., Grach, S.M., Nasyrov, I.A., and Sergeev, E.N., Spatial characteristics of the 630-nm artificial ionospheric airglow generation region during the Sura facility pumping, *Radiophys. Quantum Electron.*, 2017, vol. 60, no. 11, pp. 849–865.

Shpynev, B.G., Alsatkin, S.S., Khakhinov, V.V., and Lebedev, V.P., Investigating the ionosphere response to exhaust products of "Progress" cargo spacecraft engines on the basis of Irkutsk Incoherent Scatter Radar data, *J. Sol.-Terr. Phys.*, 2017, vol. 3, no. 1, pp. 114–127. https://doi.org/10.12737/article_58f9722a233f33.55738104

Yair, Y., Price, C., Ziv, B., et al., Space shuttle observation of an unusual transient atmospheric emission, *Geophys. Res. Lett.*, 2005, vol. 32, L02801. https://doi.org/10.1029/2004GL021551

Yang, J., Lu, G., Du, J., and Pan, W., Ground-based observations of unusual atmospheric light emissions, *J. Meteorol. Res.*, 2014, vol. 28, no. 4, pp. 624–633. https://doi.org/10.1007/s13351-014-3086-7

Zinn, J., Sutherland, C.D., Stone, S.N., Duncan, L.M., and Behnke, R., Ionospheric effects of rocket exhaust products (HEAO-C, Skylab and SPS-HLLV), DOE/NASA Satellite Power System Concept Development and Evaluation Program, *DOE*/ER-0082, 1980, pp. 1–32.

Translated by M. Chubarova